

Kinetic investigation of the anionic polymerization of MMA using sparteine as σ -ligand

François Lavaud, Michel Fontanille*, Yves Gnanou*

Laboratoire de Chimie des Polymères Organiques, ENSCPB, Université Bordeaux-1, CNRS-16, Avenue Pey-Berland, 33607 Pessac Cedex, France

Received 21 December 2001; received in revised form 9 May 2002; accepted 21 May 2002

Dedicated to the 60th birthday of Prof. Roderic Quirk

Abstract

The kinetics of the anionic polymerization of methyl methacrylate using THF as solvent, 1,1-diphenylhexyllithium as initiator and sparteine as ligand has been investigated in a flow-tube reactor for initiator concentrations higher than $1 \times 10^{-3} \text{ mol l}^{-1}$ and a temperature range between -10 and 20 °C. Addition of sparteine induced a decrease in both the reactivity of the growing enolates and the extent of termination reactions. While a fractional kinetic order relative to the active centres was obtained in the presence of sparteine, this additive shifted the equilibrium between aggregated and unimeric species toward the formation of unimeric-ligated enolates as indicated by entropic and enthalpic parameters of the aggregation equilibrium. The rate constants of propagation and termination of these growing species were also determined. © 2002 Elsevier Science Ltd. All rights reserved.

Keywords: 1,1-Diphenylhexyllithium; Anionic polymerization; Sparteine

1. Introduction

In a recent publication, we showed that the use of sparteine as an additive in the anionic polymerization of methyl methacrylate has a beneficial effect, this σ -donating ligand favouring propagation over termination through complexation with lithium, the counter-ion [1]. Polymerizations carried out in THF indeed exhibit a controlled character until -10 °C, depending on the [diamine] to [lithium] ratio used. Sparteine is a well known chiral ligand whose enantioselectivity [(–)-sparteine] was used to synthesize optically active poly(alkyl methacrylate) from racemic methacrylates in hydrocarbon solvent [2,3]. However, complexation of the ligand with the counter-ion is much weaker in THF because of the possible coordination of the latter and as a result the polymers obtained show low optical activity [4].

In other words, in the anionic polymerization of alkyl methacrylates initiated by lithiated species in THF, solvation of the counter-ion competes with a possible complexation by an additive. On the other hand, it is known that in a moderately polar medium like THF, aggregated and unimeric enolate ion pairs coexist in equilibrium as shown by Kunkel et al. [5]. Addition of a cryptand as σ -ligand

prevents the formation of aggregated species [6,7] whereas TMEDA [8] lacks sufficient power as cation-binders to entirely deaggregate the system.

Therefore, the anionic polymerization of methyl methacrylate is a complicated process where in addition to termination reactions, phenomena of solvation, complexation and aggregation must be taken into account in order to elucidate the mechanism of polymerization. NMR spectroscopy [7,9–11] and ab initio calculations [12–16] of compounds that feature the methacrylate anions have proved to be efficient tools in understanding the behaviour of ligated lithium enolate ion pairs and unveiling their structures. Additionally, kinetic studies are also powerful means for the determination of the reactivity of active species and the investigation of the influence of σ , μ , and σ/μ ligands on the propagation of ion pairs [6,8,17–22].

However, kinetic studies and the investigation of model compounds can lead to different interpretations of the structure of the ion pairs. For example, in the anionic polymerization of MMA ligated by lithium alkoxyalkoxides, different explanations of the elevated reactivity of active chain ends [22] were given using NMR spectroscopy [11] and quantum chemical studies [16]. In the anionic polymerization of MMA in toluene, a first-order kinetics with respect to the concentration in active centres was reported [23] whereas in THF where the aggregation of

* Corresponding authors.

active species is normally less acute, a fractional kinetic order was found [5]. In addition, the technique used to monitor the kinetics of polymerization seems also to matter; for instance, the rates of polymerization were found to differ between flow-tube and conventional stirred reactors in the anionic polymerization of PMMA–Na and PMMA–Cs in THF although the concentrations in monomer and initiator were the same [24,25].

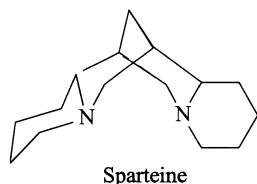
In this study, we decided to carry out our experiments in a flow-tube reactor and monitor by this means the kinetics of the anionic polymerization of MMA performed in the presence of sparteine. Even though the latter technique allows fast polymerizations to be followed, it can be efficiently applied only in a rather narrow range of initiator concentrations comprised between 1×10^{-3} and $1 \times 10^{-2} \text{ mol l}^{-1}$. The aim of this work is, therefore, to show the influence of sparteine on solvation, aggregation and complexation phenomena and determine the reactivity of the propagating enolate ion pairs when they are ligated with such a σ -donating ligand.

2. Experimental section

The kinetics in this work were all performed in a polar solvent at different temperatures with sparteine as the additive.

2.1. Reagents

MMA (Aldrich) was first stirred overnight with CaH_2 and distilled under vacuum. Then, a 10 wt% triethylaluminum/hexane solution was added drop-wise until a persistent yellowish green colour appeared. MMA was then immediately redistilled under reduced pressure just prior to polymerization. Sparteine (Aldrich) was distilled over CaH_2 and then stored under an inert nitrogen atmosphere. THF was first purified by refluxing over a fresh sodium–benzophenone complex followed by drying over a living carbanionic solution and then distilled prior to use. Octane (Aldrich) used as an internal standard was stirred over Na/K alloy, degassed and distilled under high vacuum. 1,1-Diphenylethylene (DPE) (Aldrich) was distilled over calcium hydride under reduced pressure, dried with *n*-butyllithium, and redistilled.



2.2. Initiators

The initiator, 1,1-diphenylhexyllithium (DPHLi), was

prepared by reacting the required amount of *sec*-butyllithium with a slight excess of DPE at -40°C in THF. The determination of its concentration was based to triphenylmethane/acetanilide-based double titration [26].

2.3. Polymerization kinetics

All experiments were carried out in a flow-tube reactor (Feinwerktechnik) specially designed to monitor fast polymerizations. Monomer and premixed initiator/sparteine solution were pre-cooled, efficiently mixed for less than 1 ms in a mixing jet, and allowed to pass through a capillary tube (1 mm inner diameter). The particular residence time ($5 \text{ ms} \leq \tau \leq 2 \text{ s}$) of the polymerization solution was chosen by changing the flow rate and the capillary tube length ($4 \leq l \leq 448 \text{ cm}$). The reaction mixture was deactivated at the end of the capillary tube in a quenching jet using methanol containing a small amount of acetic acid. Temperatures of the mixing jet (T_{mx}) and the quenching jet (T_{q}) were determined by using thermocouples. In each run, the flow rate was carefully chosen in order to maintain a turbulent flow throughout the polymerization with a characteristic Reynolds number, $Re > 3000$.

Experiments were carried out at T_{mx} ranging between -10 and 20°C . The effective temperature of each experiment was determined using the equation [27]

$$T_{\text{eff}} = T_{\text{mx}} + 0.55\Delta T$$

ΔT representing the temperature rise between the mixing and quenching jets. Since the polymerization is very fast, heat transfer through the walls of the tube is negligible, leading to nearly adiabatic behaviour. Temperature was corrected for each kinetic point to account for an increase resulting from monomer conversion. The temperature of mixing jet was, therefore, adjusted for all experiments in order to compensate for the exothermic nature of the polymerization and to maintain constant T_{eff} for each conversion.

2.4. Characterizations

Monomer conversion was determined using gas chromatography with octane as an internal standard. Polymers were analysed by size exclusion chromatography (SEC) using a Varian apparatus equipped with refractive index/UV dual detection and TSK gel columns with THF as eluent. Standard poly(methyl methacrylate) samples were used to plot a SEC calibration curve.

3. Results and discussion

The anionic polymerization of MMA was carried out in a flow-tube reactor with sparteine as additive and initiator concentrations ($[\text{DPHLi}]_0$) higher than $1 \times 10^{-3} \text{ mol l}^{-1}$. As previously observed from experiments carried out in a

Table 1

Characterization data for PMMA synthesized by anionic polymerization in the presence of sparteine as chelating agent in THF using a flow-tube reactor

Run	T (°C)	$[MMA]_0$ (mol l ⁻¹)	$[DPHLi]_0$ ($\times 10^3$) (mol l ⁻¹)	r'^a	$x_{p,max}^b$	$\bar{M}_{n,th}^c$ at $x_{p,max}$	$\bar{M}_{n,SEC}$ at $x_{p,max}$	\bar{M}_w/\bar{M}_n at $x_{p,max}$	f^d
S1	-10.5	0.04	1	2	0.36	1440	2130	1.14	0.71
S2	-9.7	0.1	1	2	0.39	3900	4820	1.20	0.77
S3	-9.7	0.2	1	2	0.36	7210	9720	1.26	0.72
S4	-9.0	0.4	1	2	0.38	15,220	21,160	1.24	0.73
S5	-10.2	0.2	2	0	0.54	5410	6780	1.35	0.81
S6	-9.8	0.2	2	0.5	0.58	5810	7330	1.28	0.82
S7	-9.5	0.2	2	2	0.55	5510	6650	1.21	0.88
S8	-10.8	0.2	3	2	0.60	4000	4800	1.10	0.85
S9	-11.2	0.2	5	2	0.75	3000	3250	1.13	0.90
S10	-10.3	0.2	9	2	0.85	1890	2260	1.12	0.86
S11	-6.0	0.2	5	2	0.81	3240	3980	1.12	0.86
S12	0.3	0.2	1	2	0.45	9010	12,120	1.33	0.74
S13	0.0	0.2	2	2	0.57	5710	7670	1.25	0.75
S14	-0.3	0.2	5	0	0.78	3120	3980	1.28	0.77
S15	-0.1	0.2	5	0.5	0.82	3280	4370	1.22	0.76
S16	0.2	0.2	5	0.9	0.80	3360	4600	1.14	0.73
S17	-0.6	0.2	5	2	0.84	3360	3710	1.17	0.86
S18	0.7	0.2	5	14	0.76	3040	4830	1.17	0.69
S19	-1.1	0.2	9	2	0.89	1980	2560	1.14	0.79
S20	0	0.2	11	2	0.95	1730	2060	1.16	0.84
S21	5.2	0.2	5	2	0.82	3280	4520	1.19	0.80
S22	9.9	0.2	1	2	0.36	7210	10,540	1.41	0.65
S23	10.7	0.2	2	2	0.59	5900	8860	1.32	0.72
S24	11.5	0.2	5	2	0.82	3280	4050	1.27	0.86
S25	11.6	0.2	6	2	0.87	2900	3420	1.17	0.86
S26	10.5	0.2	11	2	0.95	1730	2390	1.14	0.87
S27	16.8	0.2	5	2	0.77	3080	3710	1.32	0.70

Maximum residence time, $t_{max} = 1.932$ s.^a $r' = [\text{sparteine}]/[\text{DPHLi}]_0$.^b Conversion obtained at $t_{max} = 1.932$ s.^c $\bar{M}_{n,th} = ([M]_0/[DPHLi]_0)(x_p) \times 100.12$.^d Initiator efficiency, f , is obtained by taking the ratio of $\bar{M}_{n,th}$ to those really measured (Figs. 3 and 4).

conventional stirred reactor, sparteine has a beneficial effect on the control of the propagating process [1]. Results obtained by the flow-tube reactor are listed in Tables 1 and 2 (Exp. S5–S7 and S14–S18) and are represented in Fig. 1 for polymerizations at 0 °C and $[DPHLi]_0 = 5 \times 10^{-3}$ mol l⁻¹ with various amounts of sparteine. Upon increasing the ratio of sparteine with respect to the initiator concentration, the

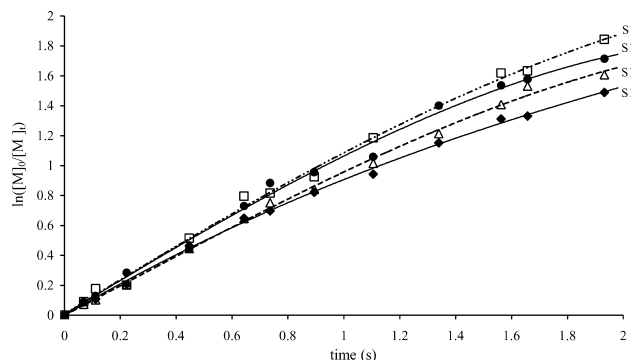


Fig. 1. First-order time conversion plots for the polymerization of MMA in THF in the presence of various amounts of sparteine and at 0 °C. $[MMA]_0 = 0.2$ mol l⁻¹, $[DPHLi]_0 = 5 \times 10^{-3}$ mol l⁻¹, $[\text{sparteine}]/[\text{DPHLi}]_0 = 0$ (◆), 0.5 (●), 0.9 (△), 2 (□).

downward trend of the $\ln([M]_0/[M]_t)$ versus time curve eventually rises up into a straight line. The non-linearity of the semilogarithmic time-conversion plot indicates that the relative polymerization rate, r_p , decreases during the reaction due to a partial deactivation of active centres, a phenomenon resulting from the occurrence of unimolecular termination reactions competing with propagation. The expression for the rate of polymerization, which accounts for these unimolecular terminations is given by the equation

$$\ln \frac{[M]_0}{[M]_t} = \frac{r_p}{k_t} (1 - e^{-k_t t}) \quad (1)$$

where $r_p = k_p[P^*]_0$, the relative polymerization rate, is the initial slope of the first-order time/conversion plot, k_p and k_t being the rate constants of propagation and termination, respectively. $[P^*]_0 = f[DPHLi]_0$ represents the actual concentration of active centres, f being the efficiency of the initiation step. The values of r_p and k_t were determined by using Eq. (1) and a least-square method that allowed all of the data points corresponding to one experiment to fit into the same curve.

The presence of sparteine also profoundly affects the molar mass distribution (Fig. 2), the resulting polymers

Table 2

Kinetic data for the anionic polymerization of MMA in the presence of sparteine as chelating agent in THF using a flow-tube reactor

Run	T (°C)	$[MMA]_0$ (mol l ⁻¹)	$10^3 \times [P^*]_0$ (mol l ⁻¹)	r^a	r_p (s ⁻¹)	$k_{p,app} = r_p/[P^*]_0$ (l mol ⁻¹ s ⁻¹)	$r_p/[P^*]_0^{1/2}$	k_t^b (s ⁻¹)	$x_{p,th}^c$
S1	-10.5	0.04	0.71	2.8	0.284	402	10.69	0.202	0.75
S2	-9.7	0.1	0.76	2.6	0.285	373	10.30	0.219	0.73
S3	-9.7	0.2	0.72	2.8	0.290	406	10.85	0.256	0.68
S4	-9.0	0.4	0.73	2.7	0.302	411	11.15	0.242	0.71
S5	-10.2	0.2	1.61	0	0.530	329	13.18	0.405	0.73
S6	-9.8	0.2	1.63	0.6	0.517	317	12.81	0.208	0.92
S7	-9.5	0.2	1.75	2.3	0.460	263	11.00	0.124	0.98
S8	-10.8	0.2	2.54	2.4	0.612	241	12.14	0.265	0.90
S9	-11.2	0.2	4.49	2.2	0.783	174	11.69	0.080	1
S10	-10.3	0.2	7.74	2.3	1.030	133	11.71	0.066	1
S11	-6.0	0.2	4.30	2.3	0.990	230	15.10	0.173	1
S12	0.3	0.2	0.74	2.7	0.491	664	18.05	0.644	0.41
S13	0.0	0.2	1.50	2.7	0.688	459	17.76	0.526	0.59
S14	-0.3	0.2	3.87	0	1.143	295	18.37	0.408	0.94
S15	-0.1	0.2	3.80	0.7	1.215	320	19.71	0.311	0.98
S16	0.2	0.2	3.63	1.2	1.131	312	18.77	0.297	0.98
S17	-0.6	0.2	4.31	2.3	1.222	284	18.61	0.257	0.99
S18	0.7	0.2	3.47	20.3	0.932	269	15.82	0.260	0.97
S19	-1.1	0.2	7.07	2.5	1.513	214	17.99	0.282	0.97
S20	0.0	0.2	9.21	2.4	1.793	195	18.68	0.169	1
S21	5.2	0.2	4.12	2.5	1.309	318	20.39	0.537	0.91
S22	9.9	0.2	0.65	3.1	0.519	798	20.36	1.043	0.40
S23	10.7	0.2	1.43	2.8	0.925	642	24.38	0.985	0.60
S24	11.5	0.2	4.31	2.3	1.520	353	23.15	0.666	0.90
S25	11.6	0.2	5.19	2.3	1.640	316	22.76	0.447	0.97
S26	10.5	0.2	9.58	2.3	2.243	234	22.92	0.394	1
S27	16.8	0.2	3.52	2.8	1.572	447	26.50	1.062	0.77

^a $r = [\text{sparteine}]/[P^*]_0$.^b Rate constant of termination, k_t , calculated using Eq. (1).^c Theoretical maximum conversion calculated using Eq. (10).

displaying a low polydispersity index ($I_p = \bar{M}_w/\bar{M}_n = 1.17$ at $x_{p,max} = 0.84$) at 0 °C. An equimolar ratio of [sparteine] to the [initiator] is essential to obtain a good control of the polymerization, the best result being actually obtained with a 2:1 excess of the ligand. Increasing further that ratio ($r = 14$) did not help to significantly improve the control of polymerization. An even better control of the molar masses

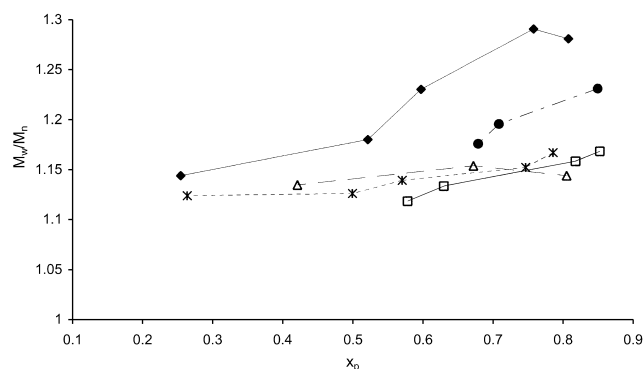


Fig. 2. Variation of polydispersity index versus conversion of PMMA obtained in THF in the presence of various amounts of sparteine and at 0 °C. $[MMA]_0 = 0.2 \text{ mol l}^{-1}$, $[DPHLi]_0 = 5 \times 10^{-3} \text{ mol l}^{-1}$, $[\text{sparteine}]/[DPHLi]_0 = 0$ (◆), 0.5 (●), 0.9 (△), 2 (□), 14 (✱).

requires much higher ratio of ligand of active species ($r = 30$ to 70) [1]. On the other hand, Figs. 3 and 4 indicate a linear dependence between the number average molar masses and the degree of conversion at various initial monomer and initiator concentrations, indicating an absence of transfer reactions. The small deviation from the theoretical line is due to the initiator efficiency, f , which

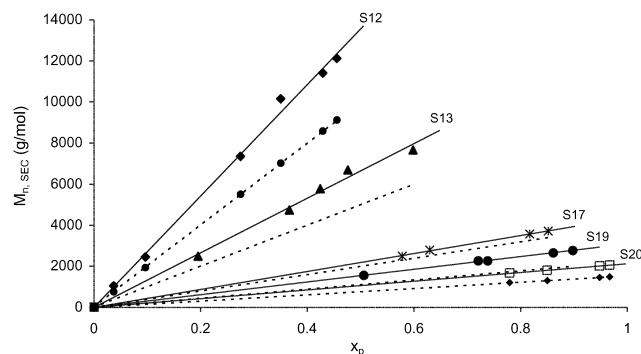


Fig. 3. Dependence of $\bar{M}_{n,SEC}$ with conversion for the polymerization of MMA in THF in the presence of a 2-fold molar excess of sparteine with respect to initiator concentration and at 0 °C. $[MMA]_0 = 0.2 \text{ mol l}^{-1}$, $[DPHLi]_0 = 11 \times 10^{-3}$ (□), 9×10^{-3} (●), 5×10^{-3} (✱), 2×10^{-3} (▲), 1×10^{-3} (◆) mol l⁻¹. (---) theoretical lines.

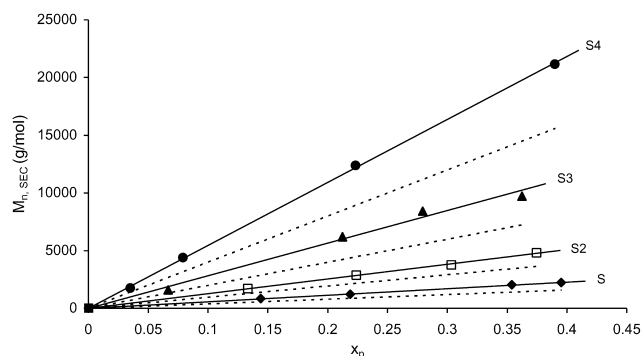


Fig. 4. Dependence of $\bar{M}_{n,SEC}$ with conversion for the polymerization of MMA in THF in the presence of a 2-fold molar excess of sparteine with respect to monomer concentration and at $-10\text{ }^{\circ}\text{C}$. $[\text{DPHLi}]_0 = 1 \times 10^{-3}\text{ mol l}^{-1}$, $[\text{MMA}]_0 = 0.4$ (●), 0.2 (▲), 0.1 (□), 0.04 (◆) mol l^{-1} . (---) theoretical lines.

is always lower than unity. All values of f are listed in Table 1 and demonstrate that initiator efficiency remains constant with or without the ligand.

3.1. Effect of reagents concentration

To determine the mechanism that prevails in such ligated anionic polymerization of MMA in THF, the external kinetic orders with respect to both monomer and active centres concentrations were calculated. From the expression of the initial rate of polymerization

$$R_{p0} = k_p [\text{P}^*]_0^\alpha [\text{M}]_0^\beta \quad (2)$$

where k_p is the rate constant of propagation, α and β the kinetic order in active centres and in monomer, one can easily deduce the respective kinetic orders on writing the following logarithmic relation

$$\ln R_{p0} = \ln k_p + \alpha \ln [\text{P}^*]_0 + \beta \ln [\text{M}]_0 \quad (3)$$

A straight line from the $\ln(R_{p0})$ versus $\ln([\text{M}]_0)$ plot for initial concentrations on monomer ranging from 0.04 to 0.2 mol l^{-1} was actually obtained (Fig. 5). As this slope is equal to unity, it can be inferred that the polymerization obeys a first-order kinetics with respect to the monomer.

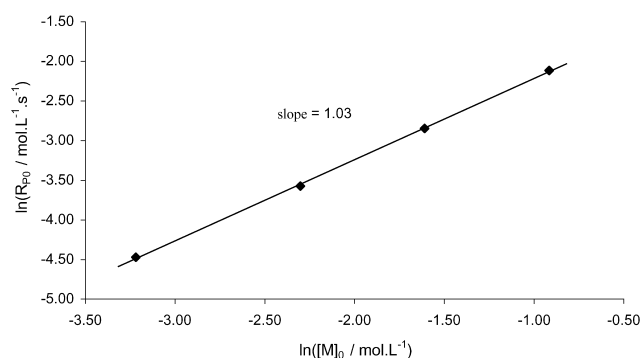


Fig. 5. Kinetic order with respect to monomer concentration for the polymerization of MMA in the presence of sparteine in THF at $-10\text{ }^{\circ}\text{C}$.

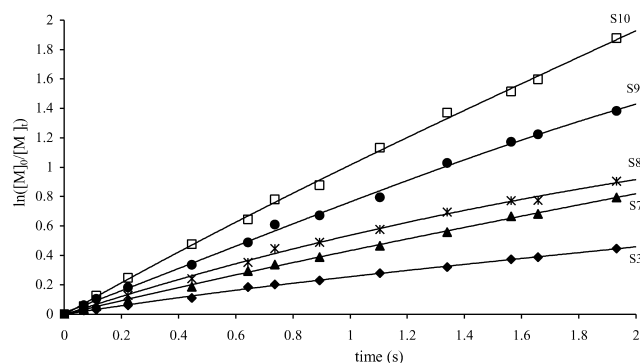


Fig. 6. First-order time conversion plots for the polymerization of MMA in THF in the presence of a 2-fold molar excess of sparteine with respect to initiator concentration at $-10\text{ }^{\circ}\text{C}$. $[\text{MMA}]_0 = 0.2\text{ mol l}^{-1}$, $[\text{DPHLi}]_0 = 9 \times 10^{-3}$ (□), 5×10^{-3} (●), 3×10^{-3} (*), 2×10^{-3} (▲), 1×10^{-3} (◆) mol l^{-1} .

The determination of the external kinetic order with respect to the active centres was performed for initiator concentrations ranging from 1×10^{-3} to $11 \times 10^{-3}\text{ mol l}^{-1}$ at several temperatures (Figs. 6–8). The bi-logarithmic r_p versus $[\text{P}^*]_0$ plot (Fig. 9) is linear. The slope is equal to 0.5 at all temperatures and suggests that a predominant fraction of active centres are aggregated. Similar fractional order was obtained by Müller et al. for the polymerization of MMA in THF whether in presence or absence of TMEDA as ligand and reflects the existence of an equilibrium between aggregated dimers and unimeric species [8]. Consequently, the rate constant of propagation calculated from the $\ln[\text{M}]_0/[\text{M}]$ versus time is only an apparent value and depends on the initiator concentration. Its expression can be written as

$$k_{p,app} = \delta k_{p\pm} + [(1 - \delta)/2]k_{pa} \quad (4)$$

where δ is the fraction of unimeric species, $k_{p\pm}$ and k_{pa} being the rate constants of unimeric species and dimeric aggregates, respectively.

From the relation of the equilibrium constant of

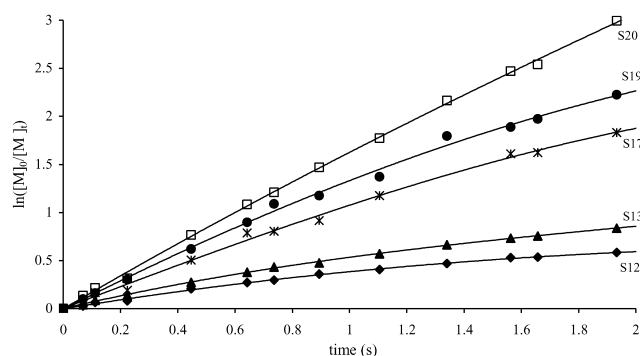


Fig. 7. First-order time conversion plots for the polymerization of MMA in THF in the presence of a 2-fold molar excess of sparteine with respect to initiator concentration at $0\text{ }^{\circ}\text{C}$. $[\text{MMA}]_0 = 0.2\text{ mol l}^{-1}$, $[\text{DPHLi}]_0 = 11 \times 10^{-3}$ (□), 9×10^{-3} (●), 5×10^{-3} (*), 2×10^{-3} (▲), 1×10^{-3} (◆) mol l^{-1} .

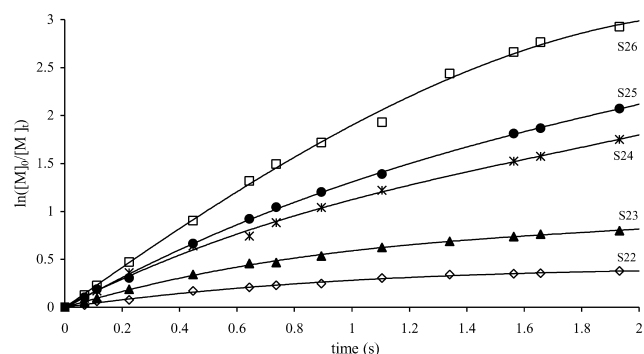


Fig. 8. First-order time conversion plots for the polymerization of MMA in THF in the presence of a 2-fold molar excess of sparteine with respect to initiator concentration at 10 °C. $[MMA]_0 = 0.2 \text{ mol l}^{-1}$, $[DPHLi]_0 = 11 \times 10^{-3}$ (□), 6×10^{-3} (●), 5×10^{-3} (*), 2×10^{-3} (▲), 1×10^{-3} (◆) mol l^{-1} .

aggregation ($K_a = [P_a^*]/[P_{\pm}^*]^2$) where $[P_a^*]$ and $[P_{\pm}^*]$ are the concentrations of dimeric aggregates and unimeric ion pairs, the fraction of 'free' species can be expressed as

$$\delta = \frac{-1 + (1 + 8K_a[P^*])^{1/2}}{4K_a[P^*]} \quad (5)$$

with

$$[P^*] = [P_{\pm}^*] + 2[P_a^*]$$

For elevated equilibrium constants of aggregation ($K_a[P^*] \gg 1$), the proportion of unimeric species is very low ($\delta = (2K_a[P^*])^{-1/2} \ll 1$) and the apparent rate constant of propagation can be linearized leading to

$$k_{p,\text{app}} = \frac{r_p}{[P^*]} = \frac{k_{p_{\pm}}}{\sqrt{2K_a[P^*]}} + \frac{1}{2}k_{p_a} \quad (6)$$

The plot of the variation of the relative polymerization rate, r_p , versus $[P^*]_0^{-1/2}$ giving a straight line, its slope corresponds to $k_{p_{\pm}}/\sqrt{2K_a}$ and its intercept to $(1/2)k_{p_a}$ (Fig. 10). From the values obtained for k_{p_a} , it can be concluded that either the aggregated species do not propagate or their reactivity is too low to be detected. Moreover, the $k_{p_{\pm}}/\sqrt{2K_a}$ ratio is constant as indicated in

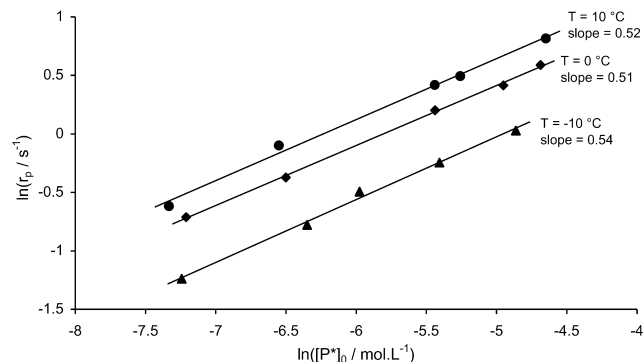


Fig. 9. Kinetic order with respect to initiator concentration for the polymerization of MMA with sparteine as ligand, in THF at -10, 0 and 10 °C.

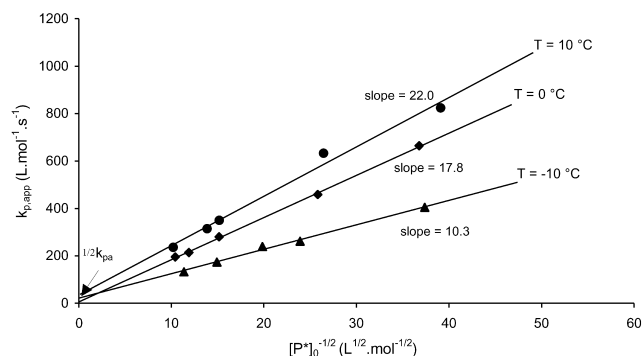


Fig. 10. Estimation of the rate constant of propagation of the dimer aggregated species in the polymerization of MMA in THF in the presence of sparteine at $T = -10, 0$ and 10 °C.

Table 2, confirming that the proportion of dimeric aggregates is elevated. The variation of the apparent rate constant of propagation versus concentration in active centres is represented in Fig. 11.

In order to gain better insight into the reactivity of the unimeric species and to what extent these enolate ion pairs themselves aggregate, Eqs. (5) and (6) can be linearized to give

$$\frac{[P^*]}{r_p} = \frac{1}{k_{p,\text{app}}} = \frac{1}{k_{p_{\pm}}} + \frac{2K_a}{k_{p_{\pm}}^2} r_p \quad (7)$$

Upon plotting the variation of $1/k_{p,\text{app}}$ versus r_p , a satisfactory straight line could be obtained (Fig. 12). The calculated absolute rate constants of unimeric species ($k_{p_{\pm}}$) which corresponds to the intercept of the lines and the equilibrium constants of aggregation (K_a) are listed in Table 3. The fraction of unimeric species depending on the concentration in active centres can be estimated. The accuracy of these values, however, must be considered as limited, as noted by Bywater in the kinetics of the anionic polymerization of styrene in hydrocarbon solvent [28]. In fact, these absolute constants fluctuate by a one-third factor within experimental error of the data points and are, therefore, mere estimations.

Another solution for determining the fractional order

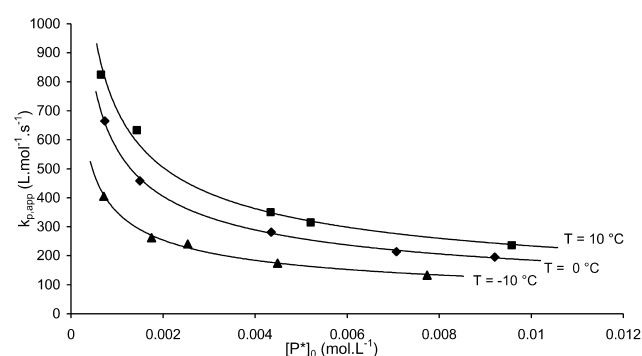


Fig. 11. Dependence of the apparent rate constant of propagation ($k_{p,\text{app}}$) on the concentration in active centres in the anionic polymerization of MMA in THF in the presence of sparteine.

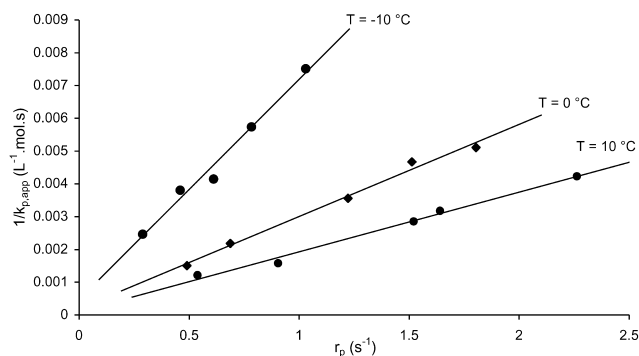


Fig. 12. Determination of the propagation rate constant of the unimeric species ($k_{p_{\pm}}$) and the equilibrium constant of aggregation (K_a) according to Eq. (6) at $T = -10, 0$ and 10 °C.

with respect to the concentration of active centres as well as $k_{p_{\pm}}$ and K_a values has been reported by Duda and Penczek [29] using Eq. (8)

$$r_p^{1-m} = -\frac{m}{K_a k_{p_{\pm}}^{m-1}} + k_{p_{\pm}} [P^*] r_p^{-m} \quad (8)$$

m being the aggregation degree. As a flow-tube reactor can only accommodate a range of initiator concentrations between 1×10^{-3} and $1 \times 10^{-2} \text{ mol l}^{-1}$, a rather low regression coefficient ($0.3 < r^2 < 0.6$) was obtained for the r_p^{-1} versus $[P^*]_0 r_p^{-2}$ plot (Fig. 13). Also, the Penczek equation only applies to truly 'living' systems: in the present case, it was utilized in the range of low to moderate conversion in order to take into account the rather limited termination observed. This may be a second reason for the low regression coefficient as shown in Fig. 13.

3.2. Activation parameters

The influence of temperature on the kinetics of polymerization was studied from -11.2 to 16.8 °C at the relatively high initiator concentration of $[DPHLi]_0 = 5 \times 10^{-3} \text{ mol l}^{-1}$ (Fig. 14). The Arrhenius plot of the apparent rate constants of propagation at this initiator concentration is shown in Fig. 15. The variation of $\ln(k_{p,app})$ versus $(1/T)$ is linear and indicates the presence of only one type of propagating active species. The activation energy and the frequency factor for the addition of a monomer molecule to a propagating ion pair PMMA–Li in THF were found equal to $E_{a,app} = 19.36 \text{ kJ mol}^{-1}$ and $\ln A_{app} = 6.13$.

These values are similar to those obtained for the anionic

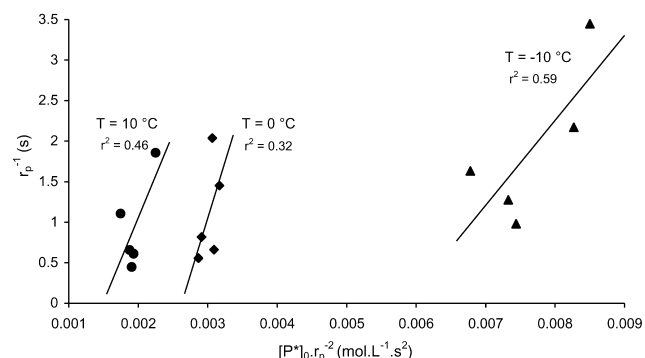


Fig. 13. Penczek's method to the determination of the propagation rate constant of the unimeric species ($k_{p_{\pm}}$) and the equilibrium constant of aggregation (K_a). (r is the linear regression coefficient).

polymerization of MMA in THF with lithium perchlorate [18] ($E_{a,app} = 20 \text{ kJ mol}^{-1}$ and $\ln A_{app} = 6.5$) or with TMEDA [8] ($E_{a,app} = 17.4 \text{ kJ mol}^{-1}$ and $\ln A_{app} = 6.1$) but they are slightly lower than those determined in the absence of additives [30] ($E_{a,app} = 24 \text{ kJ mol}^{-1}$ and $\ln A_{app} = 7.4$). However, these activation parameters are only apparent values due to their dependence on the concentration in active centres.

On the other hand, the plot of $\ln(k_{p_{\pm}})$ versus $(1/T)$ could be drawn from the $k_{p_{\pm}}$ values obtained between -10 and 10 °C and a satisfactory straight line correlation obtained ($r^2 = 0.95$) (Fig. 16). The activation energy and the frequency factor of the propagation step for unimeric species could then be determined

$$E_{a,\pm} = 33.3 \text{ kJ mol}^{-1} \text{ and } \ln A_{\pm} = 10$$

For the anionic polymerization of MMA in THF whether TMEDA was used as ligand or not, Müller et al. obtained the values of $E_{a,\pm} = 36 \text{ kJ mol}^{-1}$ and $\ln A_{\pm} = 11$ as activation parameters for unimeric species [8]. The comparison of his results with ours at $T = 0$ °C shows that the values of the rate constant of propagation ($k_{p_{\pm}}$) for the unimeric species decrease from $13,000 \text{ l mol}^{-1} \text{ s}^{-1}$ in the presence of TMEDA to $5000 \text{ l mol}^{-1} \text{ s}^{-1}$ with sparteine. These results, therefore, indicate that sparteine decreases the reactivity of the growing species.

With respect to the aggregation phenomena, the equilibrium constant of aggregation (K_a) surprisingly increases with increasing temperature (Table 3). This observation has been previously reported [8] and clearly

Table 3

Kinetic results of the rate constant ($k_{p_{\pm}}$) and fraction (δ) of the unimeric species, equilibrium constant of aggregation (K_a) in the anionic polymerization of MMA, in THF, in presence of sparteine

T (°C)	$k_{p_{\pm}}$ ($\text{l mol}^{-1} \text{ s}^{-1}$)	K_a (l mol^{-1})	$\delta [P^*]_0 = 1 \times 10^{-3} \text{ mol l}^{-1}$	$\delta [P^*]_0 = 5 \times 10^{-3} \text{ mol l}^{-1}$
-10	2100	15,400	0.16	0.08
0	5200	37,600	0.11	0.05
10	8770	70,200	0.08	0.04

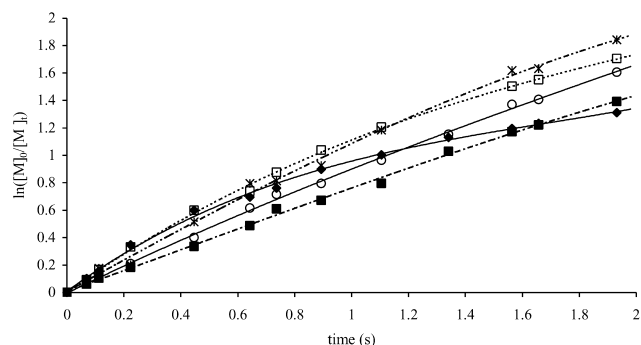


Fig. 14. First-order time conversion plots for the polymerization of MMA in THF in the presence of a 2-fold molar excess of sparteine with respect to initiator concentration at different temperatures. $[MMA]_0 = 0.2 \text{ mol l}^{-1}$, $[DPHLi]_0 = 5 \times 10^{-3} \text{ mol l}^{-1}$, $T_{\text{eff}} = -11.2$ (■), -6.0 (○), -0.6 (*), 5.2 (△), 11.5 (□), 16.8 (◆) °C.

indicates that, in the anionic polymerization of MMA in THF, aggregation is globally an endothermic process. From the values listed in Table 3, the thermodynamic parameters of the equilibrium could be determined for our system based on the use of sparteine as ligand. From the variation of $\ln(K_a)$ versus $(1/T)$ (Fig. 17), the enthalpy and entropy of aggregation could be calculated as

$$\Delta H_{\text{agg}} \approx 42 \text{ kJ mol}^{-1} \text{ and } \Delta S_{\text{agg}} \approx 240 \text{ J mol}^{-1} \text{ K}^{-1}$$

These values are higher than those obtained for the same system in the presence of TMEDA or in its absence ($\Delta H_{\text{agg}} \approx 18 \text{ kJ mol}^{-1}$ and $\Delta S_{\text{agg}} \approx 160 \text{ J mol}^{-1} \text{ K}^{-1}$); it was, therefore, inferred that TMEDA does not affect the aggregation of enolate ion pairs [8].

Wang et al. [7] have studied the influence of various σ -ligands on methyl α -lithio isobutyrate (MIBLi), a molecular model of living lithiated poly(methyl methacrylate) anions. They have established that MIBLi exists as dimeric and tetrameric aggregated species and, depending on the power of the cation-binding ligand used, the equilibrium aggregation is more or less shifted towards the formation of dimeric species.

Therefore, for the anionic polymerization of MMA in the presence of sparteine, the rather high values obtained for the

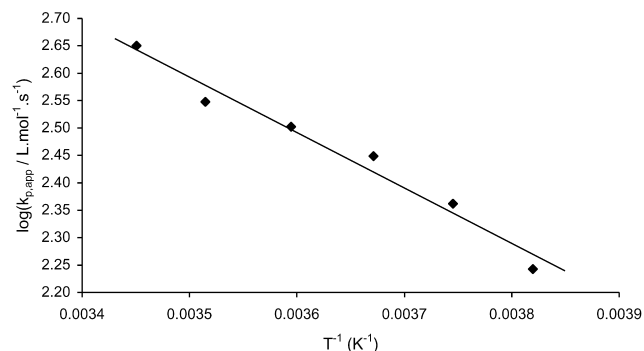


Fig. 15. Arrhenius plot of the apparent propagation rate constants ($k_{p,\text{app}}$) in the anionic polymerization of MMA in THF with sparteine as an additive ($[DPHLi]_0 = 5 \times 10^{-3} \text{ mol l}^{-1}$).

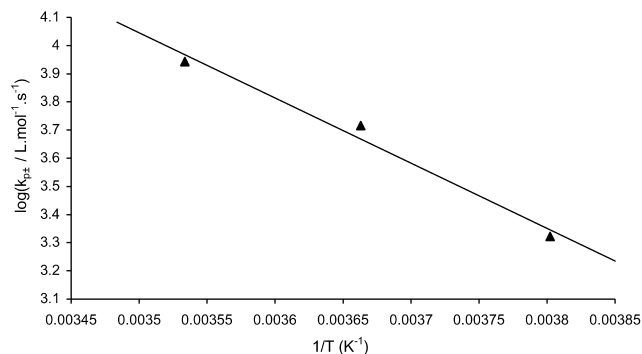


Fig. 16. Arrhenius plot of the propagation rate constants ($k_{p,\text{un}}$) of the unimeric species in the anionic polymerization of MMA in THF in the presence of sparteine.

thermodynamic parameters suggest that this additive shifts the aggregation equilibrium towards the formation of unimeric species. For a concentration in active centres equal to $1 \times 10^{-3} \text{ mol l}^{-1}$ and at -10 °C, the proportion of unimeric species is higher in the anionic polymerization of MMA in THF carried out in the presence of sparteine ($\delta \approx 0.16$) than for the same system performed with TMEDA as a ligand; δ is indeed equal to 0.13 even at the lower temperature of $T = -20$ °C [8].

The increase in the fraction of unimeric species observed in the presence of sparteine is thus compensated for by the decrease in reactivity of the corresponding unimeric ligated enolate ion pairs, a phenomenon that explains the similarity in the apparent propagation rate constants in the presence or absence of sparteine.

3.3. Unimolecular termination

The anionic polymerization of MMA in THF is affected, however, by unimolecular termination, particularly when the initiator concentration is low. Upon decreasing the initiator concentration, the semilogarithmic time-conversion plots exhibit a significant downward curvature (Figs. 6–8). The results relative to the overall rate constant of termination (k_t) are listed in Table 2 and show that k_t values increase with decreasing initiator

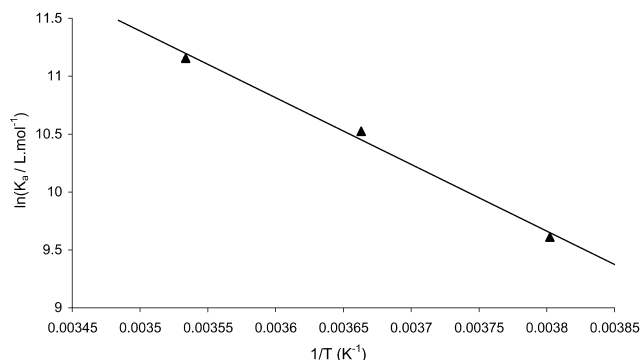


Fig. 17. Arrhenius plot of equilibrium constant of aggregation in the anionic polymerization of MMA in THF in the presence of sparteine.

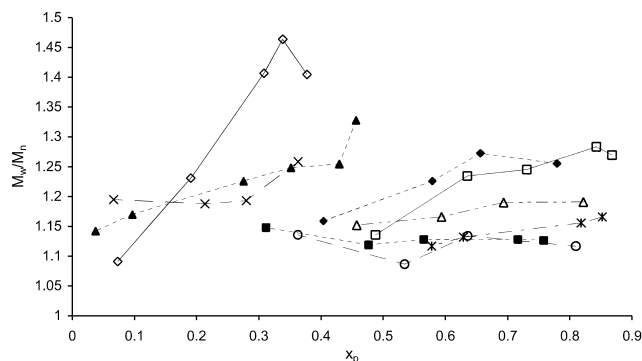


Fig. 18. Variation of polydispersity index versus conversion of PMMA obtained in the presence of sparteine at different reaction temperatures. $[MMA]_0 = 0.2 \text{ mol l}^{-1}$, $[DPHLi]_0 = 1 \times 10^{-3} \text{ mol l}^{-1}$, $T = -10$ (x), 0 (▲), 10 (◇) °C, $[DPHLi]_0 = 5 \times 10^{-3} \text{ mol l}^{-1}$, $T = -11$; 2 (■), -6.0 (○), -0.6 (✱), 5.2 (△), 11.5 (□), 16.8 (◆) °C.

concentration regardless of the temperature considered. This variation of k_t with $[P^*]_0$ indicates that the values measured are only apparent ones and suggest that the extent of termination depends on the equilibrium between dimeric and unimeric enolate ion pairs, exactly as does propagation. As these side reactions affect the final monomer conversion, the theoretical maximum conversion can be evaluated (Table 2).

Using Eq. (1), as $t \rightarrow \infty$, the limiting value of $\ln([M]_0/[M]_t)$ is given by

$$\ln \frac{[M]_0}{[M]_t} = \frac{r_p}{k_t} = \frac{[P^*]_0 k_{p,app}}{k_t} \quad (9)$$

and the maximum conversion ($x_{p,max}$) is described by the following expression

$$x_{p,max} = 1 - \exp\left(-\frac{k_{p,app}[P^*]_0}{k_t}\right) \quad (10)$$

The maximum conversion, therefore, decreases with concentration in active centres and obviously depends on the values taken by the rate constant of unimolecular termination. While termination reactions do not change the number average molar mass, they affect the mass average molar mass with an increase in the molar mass distribution for low concentrations in active centres (Fig. 18). Taking into account the existence of an equilibrium between aggregated and unimeric species, the expression of the rate constant of termination can be written as

$$k_t = \delta k_{t_{\pm}} + [(1 - \delta)/2] k_{t_a} \quad (11)$$

$k_{t_{\pm}}$ and k_{t_a} being the rate constant of termination for unimeric and aggregated enolate ion pairs. For a high enough degree of aggregation, ($K_a[P^*] \gg 1$ and $\delta = (2K_a[P^*])^{-1/2} \ll 1$), the rate constant of termination can be described by the following expression

$$k_t = \frac{1}{2} k_{t_a} + \frac{k_{t_{\pm}}}{\sqrt{2K_a[P^*]}} \quad (12)$$

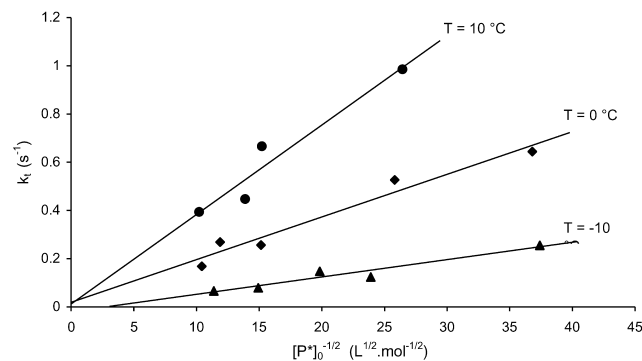


Fig. 19. Estimation of the rate constant of termination of the dimer aggregates in the anionic polymerization of MMA in THF in the presence of sparteine at various temperatures.

The variation of k_t versus $[P^*]_0^{-1/2}$ was plotted for various temperatures ($T = -10, 0, 10$ °C), yielding straight lines with a linear regression coefficient in the range of $0.93 < r^2 < 0.95$ (Fig. 19). The intercept ($1/2 k_{t_{\pm}}$) of these lines passing through the origin, it can be inferred within experimental errors that the aggregated propagating ion pairs do not undergo detectable termination reactions. Therefore, we can conclude that the rate constant of termination indirectly depends on the concentration in active centres insofar as the proportion of aggregated species decreases and the effect of termination is more pronounced at a lower initiator concentration.

Assuming that the only propagating species are those under the unimeric form, the rate constant of termination ($k_{t_{\pm}}$) could be estimated and fitted to the experimental data by using Eqs. (5) and (12) and a non-linear least-squares method. Values of $k_{t_{\pm}} = 1.20, 5.30, 14.60 \text{ s}^{-1}$ were, respectively, obtained at $T = -10, 0, 10$ °C. However, these values could not be confirmed through experiments conducted with a lower range of initiator concentrations than those used because the maximum conversion ($x_{p,max}$) in that case would have been close to zero given the high rate constants of termination.

Though aggregation phenomena are less important at elevated temperatures, the impact of termination becomes more perceivable under such conditions as indicated by a prominent downward trend in the time-conversion plots (Fig. 14). The reactivity of active chain ends and thus their propensity to termination increase with increasing temperature as expected. The Arrhenius plot of the rate constants of termination at an initiator concentration of $5 \times 10^{-3} \text{ mol l}^{-1}$ is shown in Fig. 20. From this, the activation parameters could be evaluated to be

$$E_{a,t} = 56.3 \text{ kJ mol}^{-1} \text{ and } \log A_t = 10.2$$

These values are higher than those obtained for the anionic polymerization of MMA in the absence of any ligand or even in the presence of TMEDA ($E_{a,t} = 35.5 \text{ kJ mol}^{-1}$ and $\log A_t = 6.7$) [8] and thus confirm the beneficial effect of sparteine on the control of the anionic polymerization of MMA.

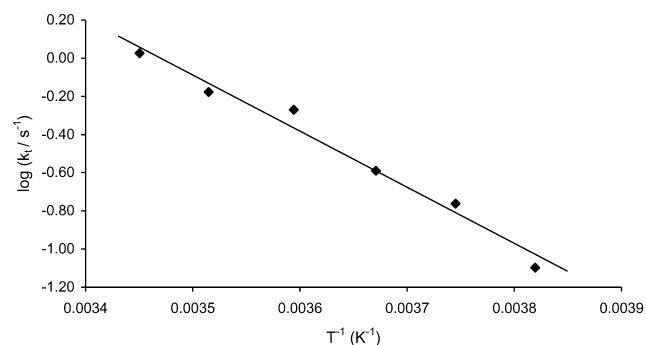


Fig. 20. Arrhenius plot of the termination rate constants (k_t) in the anionic polymerization of MMA in THF with sparteine as an additive. ($[DPHLi]_0 = 5 \times 10^{-3} \text{ mol l}^{-1}$).

3.4. Limits of a flow-tube reactor in k_t determination

In a flow-tube reactor, the exothermicity of the polymerization which is directly proportional to monomer conversion results in a rise of temperature between the mixing (T_{mx}) and quenching (T_q) jets. Fig. 21 shows examples of such temperature rise during the reactions for various monomer concentrations. Because the dissipation of heat is difficult in such short reaction times, the increase of temperature may be significant depending upon the case and the conversion considered. As a result, the system is not as isothermal as one would expect. As indicated in Section 2 and following the recommendations made by the constructor, the effective or the mean temperature in the reactor could be calculated using the relation: $T_{eff} = T_{mx} + 0.55(T_q - T_{mx})$ for each conversion. The latter was derived to compensate for the drift in temperature occurring during the polymerization; the larger the conversion in monomer, the larger the gap between T_{eff} and T_q . This feature may be responsible for a lack of precision in the determination of the values of $k_{t\pm}$, the latter being even more overestimated because the $T_q - T_{eff}$ difference is large.

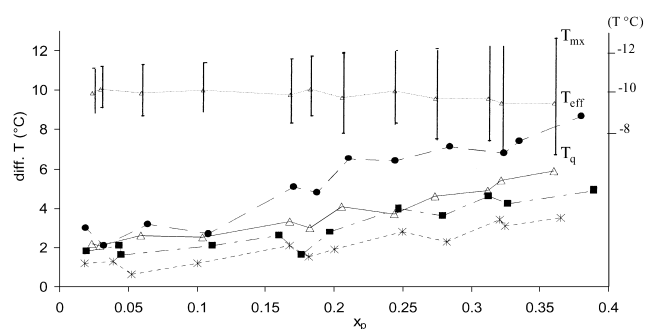


Fig. 21. Temperature rise between mixing and quenching jet in the anionic polymerization of MMA in THF using a flow-tube reactor at various monomer concentrations and at $T_{eff} = -10^\circ \text{C}$. $[DPHLi]_0 = 1 \times 10^{-3} \times \text{mol l}^{-1}$, $[MMA]_0 = 0.04$ (*), 0.1 (■), 0.2 (△), 0.4 (●) mol l^{-1} . Error bars give an overview of the mixing jet (T_{mx}) and quenching jet (T_q) for $[MMA]_0 = 0.2 \text{ mol l}^{-1}$.

4. Conclusions

Several important features can be stressed from the results of these kinetic studies.

- (1) Sparteine is an efficient additive for the anionic polymerization of MMA and generates enough steric hindrance around the growing species to reduce the extent of termination reactions.
- (2) This additive shifts the aggregation equilibrium towards unimeric ligated species which appear less reactive than unligated enolates. Due to this compensation, the apparent rate constants of propagation are similar to those obtained in the absence of any additive.
- (3) The actual rate constants of propagation ($k_{p\pm}$) and termination ($k_{t\pm}$) of the unimeric enolates were also determined. In contrast to the $k_{p\pm}$ values which are perfectly reliable as determined by the flow-tube reactor, the rate constants of termination $k_{t\pm}$ are more questionable due to the non-isothermal and non-adiabatic character of this type of equipment. A series of experiments using an adiabatic calorimeter and involving small variations in temperature is currently being carried out for comparison purpose.

References

- [1] Marchal J, Gnanou Y, Fontanille M. *Macromol Symp* 1996;107:27.
- [2] Okamoto Y, Yashima E. *Prog Polym Sci* 1990;15:263.
- [3] Liu W, Yang Y, Chen C, Chen Y, Xi F. *Macromol Chem Phys* 1997; 198:279.
- [4] Nakano T, Okamoto Y. *Macromol Rapid Commun* 2000;603:21.
- [5] Kunkel D, Müller AHE. *Macromol Symp* 1992;60:315.
- [6] Johann C, Müller AHE. *Makromol Chem Rapid Commun* 1981;2: 687.
- [7] Wang JS, Jérôme R, Warin R, Zhang H, Teyssié P. *Macromolecules* 1994;27:3377.
- [8] Baskaran D, Müller AHE, Sivaram S. *Macromol Chem Phys* 2000; 201:1901.
- [9] Wang JS, Warin R, Jérôme R, Teyssié P. *Macromolecules* 1993;26: 6776.
- [10] Wang JS, Jérôme R, Warin R, Teyssié P. *Macromolecules* 1994;27: 1691.
- [11] Wang JS, Jérôme R, Warin R, Teyssié P. *Macromolecules* 1994;27: 4896.
- [12] Yakimansky AV, Müller AHE, Van Beylen M. *Macromolecules* 2000;33:5686.
- [13] Schmitt B, Schlaad H, Müller AHE, Mathiasch B, Steiger S, Weiss H. *Macromolecules* 2000;33:2887.
- [14] Schmitt B, Schlaad H, Müller AHE, Mathiasch B, Steiger S, Weiss H. *Macromolecules* 1999;32:8340.
- [15] Yakimansky AV, Müller AHE. *J Am Chem Soc* 2001;123:4932.
- [16] Yakimansky AV, Müller AHE. *Macromolecules* 1999;32:1731.
- [17] Kunkel D, Müller AHE, Janata M, Lochmann L. *Polym Prepr (ACS Div Polym Chem)* 1991;32:301.
- [18] Baskaran D, Müller AHE, Sivaram S. *Macromolecules* 1999;32:1356.
- [19] Lochmann L, Müller AHE. *Makromol Chem* 1990;191:1657.
- [20] Schlaad H, Schmit B, Müller AHE, Jüngling S, Weiss H. *Macromolecules* 1998;31:573.
- [21] Schlaad H, Müller AHE. *Macromolecules* 1998;31:7127.

- [22] Maurer A, Marcarian X, Müller AHE, Navarro C, Vuillemin B. *Polym Prepr (ACS Div Polym Chem)* 1997;38:467.
- [23] Wiles DM, Bywater S. *Trans Faraday Soc* 1965;150:61.
- [24] Warzelhan V, Höcker H, Schulz GV. *Makromol Chem* 1978;2221:179.
- [25] Kraft R, Müller AHE, Warzelhan V, Höcker H, Schulz GV. *Macromolecules* 1978;11:1093.
- [26] Kamienski CW. *Titration methods for commercial organolithium compounds*. FMC Lithium Division; 1994.
- [27] Löhr GZ. *Phys Chem (Frankfurt am Main)* 1972;78:177.
- [28] Bywater S. *J Polym Sci, Part A: Polym Chem* 1998;36:1065.
- [29] Duda A, Penczek S. *Macromolecules* 1994;27:4867.
- [30] Jeuck H, Müller AHE. *Makromol Chem Rapid Commun* 1982;3:121.